# Genomic mechanisms of evolved physiological plasticity in killifish distributed along an environmental salinity gradient

**Andrew Whitehead[1], Jennifer L. Roach, Shujun Zhang, and Fernando Galvez**

Department of Biological Sciences, Louisiana State University, Baton Rouge, LA 70803

Edited* by George N. Somero, Stanford University, Pacific Grove, CA, and approved March 8, 2011 (received for review November 24, 2010)

**Adaptive variation tends to emerge clinally along environmental gradients or discretely among habitats with limited connectivity. However, in Atlantic killifish (*Fundulus heteroclitus*), a population genetic discontinuity appears in the absence of obvious barriers to gene flow along parallel salinity clines and coincides with a physiologically stressful salinity. We show that populations resident on either side of this discontinuity differ in their abilities to compensate for osmotic shock and illustrate the physiological and functional genomic basis of population variation in hypoosmotic tolerance. A population native to a freshwater habitat, upstream of the genetic discontinuity, exhibits tolerance to extreme hypoosmotic challenge, whereas populations native to brackish or marine habitats downstream of the discontinuity lose osmotic homeostasis more severely and take longer to recover. Comparative transcriptomics reveals a core transcriptional response associated with acute and acclimatory responses to hypoosmotic shock and posits unique mechanisms that enable extreme osmotic tolerance. Of the genes that vary in expression among populations, those that are putatively involved in physiological acclimation are more likely to exhibit nonneutral patterns of divergence between freshwater and brackish populations. It is not the well-known effectors of osmotic acclimation, but rather the lesser-known immediate-early responses, that appear important in contributing to population differences.**

adaptive acclimation | ecological genomics | microarray

Atlantic killifish (*Fundulus heteroclitus*) occupy an extremely wide osmotic niche from freshwater to marine, and populations are distributed along steep salinity gradients in Atlantic coast estuaries. In the Chesapeake Bay, salinity gradients are distributed across hundreds of kilometers, although no obvious barriers to gene flow exist across this continuum of osmotic habitats. Because salinity is arguably the most important single physical environmental variable that delimits aquatic species distributions in nature (including *Fundulus* species; ref. 1), we exploit *F. heteroclitus* distributed along Chesapeake Bay salinity gradients as a model to discover genes and pathways that enable extreme physiological plasticity and to explore the physiological and functional genomic basis of adaptive microevolution in alternative osmotic environments.

## Results and Discussion

**Population Genetic Divergence.** We characterized the genetic structure of killifish distributed along two parallel salinity gradients in Chesapeake Bay: one along the Potomac River and the other along the James River (Fig. 1*A*). Steep clines in allele frequency for both mitochondrial and nuclear markers were centered at nearly identical salinities along the parallel gradients (Fig. 1*B*). Genotype frequency clines bounded the tidal freshwater transition region (<0.5 ppt) of both rivers, where sites upstream are freshwater year-round according to 20 y of data logged from fixed monitoring stations (www.chesapeakebay.net/data_waterquality.aspx). The populations representing either end of the cline were from upstream and downstream of the tidal freshwater position for both rivers.

There is general agreement that *F. heteroclitus*, although euryhaline, prefer brackish and marine environments (2–4) and maintain a seawater-type gill morphology to near fresh water (5, 6). In seawater (SW), the apical surface of the gill epithelium is composed of pavement cells interspersed with mitochondrion-rich chloride cells that possess apical crypts with small surface areas (7, 8). Freshwater (FW) exposure causes rapid transition from a SW to FW gill morphology, characterized by an enlarged apical surface of mitochondrion-rich cells. Copeland (5) reported that gills of *F. heteroclitus* transitioned from a SW to a FW phenotype at some salinity <1/16th SW (≈1 ppt). Consistent with this report, we find that fish from upstream of the genetic discontinuity (P1 population) have a mixed SW and FW gill morphology at 0.4 ppt, but have transitioned to a predominantly FW morphology at 0.1 ppt (Fig. S1). In contrast, fish from downstream of the genetic discontinuity (P6 and VC populations) retain a predominantly SW morphology at 0.4 ppt, but transition to a predominantly FW morphology at 0.1 ppt. Although subtle population variation exists, these data indicate that salinities <1.0 ppt represent a physiological threshold. This SW-to-FW transition is energetically expensive, costing killifish up to 10% of their total energy budget (9, 10).

The abrupt genetic discontinuity, which appears without obvious barriers to gene flow and bounds the same salinity along parallel gradients, is suggestive of nonneutral evolutionary divergence. Given that salinities <1 ppt are physiologically stressful and require an energetically expensive morphological and physiological transition, we propose that populations resident on either side of this environmental boundary have evolved adaptations specific to their osmotic niche (FW or brackish), and that this limits gene flow across the salinity boundary of ≈0.5 ppt. Indeed, relationships between environmental salinity and population divergence in the absence of obvious barriers to gene flow appear in other estuarine species (e.g., refs. 11 and 12). To test this hypothesis, and to explore mechanisms underlying adaptive acclimation, we compared physiological and transcriptomic responses to hypoosmotic challenges among common-gardened populations of *F. heteroclitus* collected from three sites spanning the salinity gradient in Chesapeake Bay: one population from FW upstream of the population genetic discontinuity (Potomac River, site 1; "P1"), a second population from downstream of the population genetic discontinuity at a mesohaline site in the middle of Chesapeake Bay ("P6"), and finally a marine population from coastal Virginia ("VC") (Fig. 1*A*).

Putatively neutral nuclear markers were used to estimate the genetic distance separating experimental populations and to es-

Author contributions: A.W. and F.G. designed research; A.W., J.L.R., S.Z., and F.G. performed research; A.W., S.Z., and F.G. analyzed data; and A.W. and F.G. wrote the paper.

The authors declare no conflict of interest.

Database deposition: Microarray data are deposited in the ArrayExpress Archive (accession no. E-MTAB-524).

*This Direct Submission article had a prearranged editor.

[1]To whom correspondence should be addressed. E-mail: andreww@lsu.edu.

This article contains supporting information online at www.pnas.org/lookup/suppl/doi:10.1073/pnas.1017542108/-/DCSupplemental.

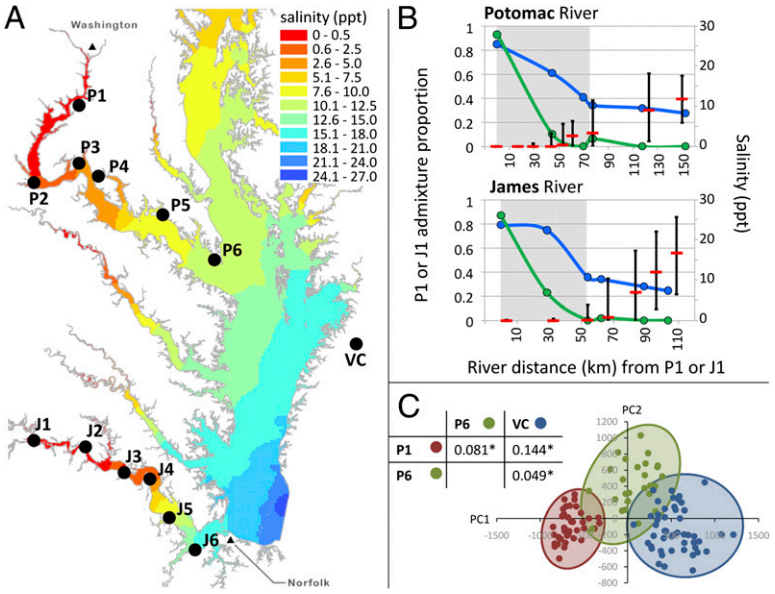


**Fig. 1.** Population genetic clines across parallel salinity gradients in Chesapeake Bay. (*A*) Map shows sampling locations along both the Potomac River (P1–P6) and James River (J1–J6). Heat overlay indicates 20-y (1986–2005) average salinity (ppt). (*B*) Line graphs show clines in admixture proportions for microsatellite (blue line) and mitochondrial (green line) markers plotted against river distance from the most extreme upper-estuary population (P1 or J1). Red points with black bars indicate 20-y average salinity and range for fixed sampling locations. (*C*) Cluster diagram illustrates multilocus microsatellite genotype divergence of individuals after principal components analysis for populations used for experiments including P1 (freshwater; red points), P6 (meso-haline; green points), and VC (coastal marine; blue points), and table reports pairwise genetic distance (Cavalli-Sforza and Edwards' chord distance) between populations (star indicates statistical significance, $P < 0.001$, permutation test).

tablish an expected covariance matrix used to interpret results from comparative experiments. The three experimental populations are genetically distinct ($P < 0.001$ for pairwise $F_{ST}$) and the divergence pattern indicates "isolation-by-distance," insofar as the two most geographically distant populations (P1 and VC) are most genetically distant, and neighboring populations are separated by intermediate genetic distance (Fig. 1*C*). This pattern of neutral genetic divergence establishes a matrix of expected covariances among other population traits. For example, if physiological differences among populations are caused by neutral evolutionary processes, then one would expect that the physiologies of the most genetically distant populations to be most different and physiologies of neighboring populations to be more similar to each other.

**Physiological Divergence.** Comparative physiological challenge experiments indicate population divergence that rejects our neutral model of isolation by distance and favors our alternative hypothesis that the population native to FW has adaptively diverged from our two SW-inhabiting populations. Fish collected from sites P1, P6, and VC were common-gardened to 32 ppt in recirculating aquarium systems, challenged with hypoosmotic conditions, and physiological and gene expression responses were tracked during acclimation. Fish challenged down to 5 ppt, and 0.4 ppt did not lose osmotic balance at any time during the acclimation time-course (Fig. 2), representing enormous physiological plasticity. When challenged down to 0.1 ppt, the two SW-derived populations (P6 and VC) lost plasma osmotic balance more severely and for significantly longer ($P < 0.001$) than the FW population. That is, the FW-derived population is more tolerant of hypoosmotic challenge than both SW-derived populations, which responded identically. This result rejects our neutral expectation but is consistent with our hypothesis of adaptive divergence. We propose that euryhaline *F. heteroclitus* is essentially a marine teleost that maintains a SW gill morphology to very low environmental salinities approaching FW. Although all populations retain the potential for hypoosmotic acclimation, those resident in exclusively FW environments exhibit adaptive divergence in compensatory responses to very low salinity.

**Transcriptional Divergence.** Gene expression was measured in gill tissues (the primary osmoregulatory tissue in fish; ref. 13) by using custom microarrays (14). Gene expression variation was characterized throughout the acclimation time-course and among populations, and patterns of population divergence were assigned to alternate evolutionary models: a putatively neutral model where population divergence in gene expression matches our isolation-by-distance expectation (Fig. 1) and a putatively adaptive model that matches population divergence in gene expression to the pattern of population divergence in physiology where the freshwater population (P1) is the outlier (Fig. 2). These data were used to identify the core transcriptional response underlying the extreme physiological plasticity observed and to implicate physiological mechanisms that contribute to evolved physiological divergence among populations.

A general linear model was used to identify genes with expression associated with acclimation and population divergence by specifying "time" and "population" as main effects, including an interaction term. A time effect was detected for 826 genes ($P < 0.01$, FDR = 0.01), a population effect for 874 genes ($P < 0.01$, FDR = 0.01), and population-dependent time effect

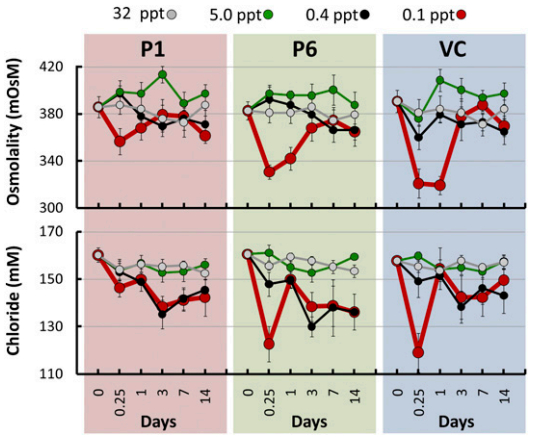


**Fig. 2.** Changes in plasma osmotic homeostasis during acclimation after hypoosmotic challenge. Fish were acclimated to 32 ppt, sampled before transfer (time 0) then challenged with low salinities 5 ppt (green line), 0.4 ppt (black line), and 0.1 ppt (red line), including a 32 ppt control transfer (gray line), and sampled 6 h, 24 h, 3 d, 7 d, and 14 d after transfer. Blood plasma was used to measure mean osmolality (mOsM; *Upper*) and mean chloride (mM; *Lower*) from $n = 6$ replicate fish sampled per time per salinity from each of 3 populations (P1, red; P6, green; VC, blue). Bars represent SEs.

(interaction) for 316 genes ($P < 0.01$, FDR = 0.05) (Fig. S2). Results from statistical tests are reported for all genes in Dataset S1. We focused on three sets of genes. The first set is those showing a time effect only. These 508 genes are more likely to be functionally involved in enabling acclimation compared with genes that do not change in expression through time, and because this set does not vary in expression across populations, genes within this set represent the core acclimation response. The second set is those showing a population effect only. These 560 genes do not vary in expression across time, so they are less likely to be functionally involved in the acclimation response, and just vary in constitutive levels of expression across populations. The third set is those that show a population and a time effect (217 genes) or an interaction effect (316 genes). These genes vary with time so they are likely to be functionally involved in acclimation, but the time response varies across populations. This set of genes is likely to offer insight into physiological and biochemical mechanisms that contribute to, or reflect, evolved differences in osmotic acclimation abilities among experimental populations.

**Core Transcriptional Response Genes.** The genes with trajectories of expression change through the acclimation time-course that are identical across populations (Fig. 3) reflect the core transcriptional response enabling hypoosmotic acclimation. The first principal component summarizing transcriptome variation accounts for 36% of the variation (Fig. 3*A*), tracks primarily a linear trajectory through principal component (PC) space, and is highly correlated with coregulated gene sets 1 (genes up-regulated through acclimation) and 4 (genes down-regulated through acclimation) (Fig. 3*B*). The second principal component accounts for 17% of the variation (Fig. 3*A*), tracks a reversible trajectory through PC space, and is highly correlated with coregulated gene sets 2 (genes transiently up-regulated) and 3 (genes transiently down-regulated) (Fig. 3*B*).

The up-regulated set is largely enriched for genes involved in energy metabolism, including components of oxidative phosphorylation, glycolysis, TCA cycle, and lipid metabolism pathways, and creatine kinase. These results are consistent with the energy expenditure necessary to transition from a SW to FW physiology (9, 10).

One of the most dramatically up-regulated genes in gills is otopetrin 1 (OTOP1), increasing in expression >20-fold, yet its role is osmoregulation has not been reported (Fig. 3*C*). Morpholino knockdown prevents otolith development in zebrafish (15), and this protein has been reported to regulate intracellular calcium (16). According to Hughes et al. (16), OTOP1 may function "as a novel ATPase or ATP-requiring transporter, or as a $Ca^{2+}$ pump or an ion exchanger," yet the gene exhibits no homology with any known ion channels, which is particularly intriguing given that cation channels important for osmoregulation in FW have been experimentally predicted but not yet found in teleost genomes (17). Additionally, intracellular $Ca^{2+}$ is, among many functions, important for activating osmolyte channels, and many additional genes that bind $Ca^{2+}$ are also up-regulated concurrent with OTOP1 (Fig. 4*C*).

The largest coregulated set of core genes are transiently up-regulated, where expression increases early in the hypoosmotic acclimation time-course (by 6–24 h) but returns to pretransfer levels by 7 d (Fig. 3*B*, set 2). Within this set of genes, the subset with highest correlation of time-course responses across populations (average pairwise correlation >80%; $P < 0.01$) is enriched for ontology terms including "cell-cell adhesion" and "nucleosome." The cell-cell adhesion cluster includes proteins that form and regulate the tight-junction paracellular space, including the claudins and occludins (Fig. 3*D*). In fish gill, epithelial tight junctions regulate paracellular ion loss (18, 19), and killifish acclimation to FW involves constriction of this paracellular pathway and alteration of the charge selectivity of tight-junction proteins to regulate the relative efflux of ions at the gills (4, 20). Because of their limited active chloride uptake in FW, *F. heteroclitus* is required to limit chloride efflux after transition to FW (20). Scott et al. (21) proposed that reducing the paracellular loss of chloride was a probable mechanism contributing to population variation in FW tolerance in *F. heteroclitus*. The strong coordinated regulation of these genes in the gill is consistent with the immediate challenge of regulating paracellular ion loss when challenged with a hypoosmotic environment (22, 23).

Histone genes also show coordinated transient up-regulation (Fig. 3*E*), although the functional relevance of this response during hypoosmotic acclimation is not clear. Chromatin is more peripherally distributed in the nucleus of FW cell types in *F. heteroclitus* (24), which may enable cells to transcriptionally respond more quickly to environmental cues (25). Also, it is possible that the immediate crisis of cell swelling upon hypoosmotic challenge triggers cellular protective responses that serve to maintain chromatin structure and chromosomal stability that involves regulation of these nucleosome proteins.

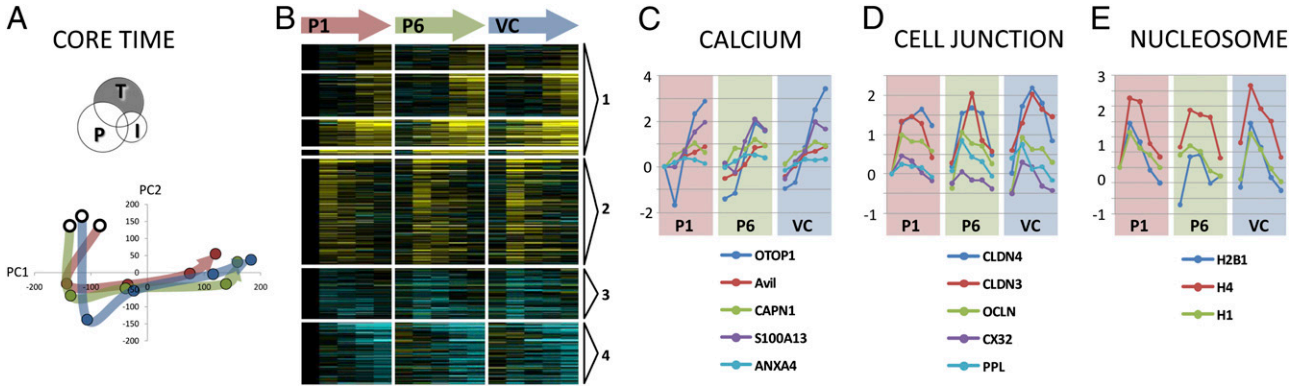


**Fig. 3.** Core acclimation-enabling gene expression patterns. (*A*) Transcriptome trajectories through principal component space (PC1 and PC2 on *x* and *y* axis, respectively) for the set of genes with a statistical time effect only (Venn diagram). Arrow base starts at time 0 h and progresses through to 168 h. (*B*) Heat map where each row represents expression level of a gene and each column a time-by-population treatment ($n = 5$ replicate fish). The first block of five columns represent the time-course (0, 6, 24, 72, and 168 h in consecutive columns) for population P1 (red arrow), and the second and third blocks for populations P6 (green arrow) and VC (blue arrow), respectively. Cell heat represents average expression level ($n = 5$ replicate fish) normalized to zero in population P1 time 0, where yellow and blue represent relative up- and down-regulation. Coregulated genes sets are numbered 1 (up-regulated), 2 (transiently up-regulated), 3 (transiently down-regulated), and 4 (down-regulated). (*C*, *D*, and *E*) Line graphs of average expression for individual genes (highlighted in the text) for each population (P1, P6, and VC represented by red, green, and blue, respectively) through consecutive time-points (starting at 0 h on the left, finishing at 168 h on the right, for each line), where *y* axis units represent $\log_2$-fold change in expression (each 1 unit = twofold expression change).

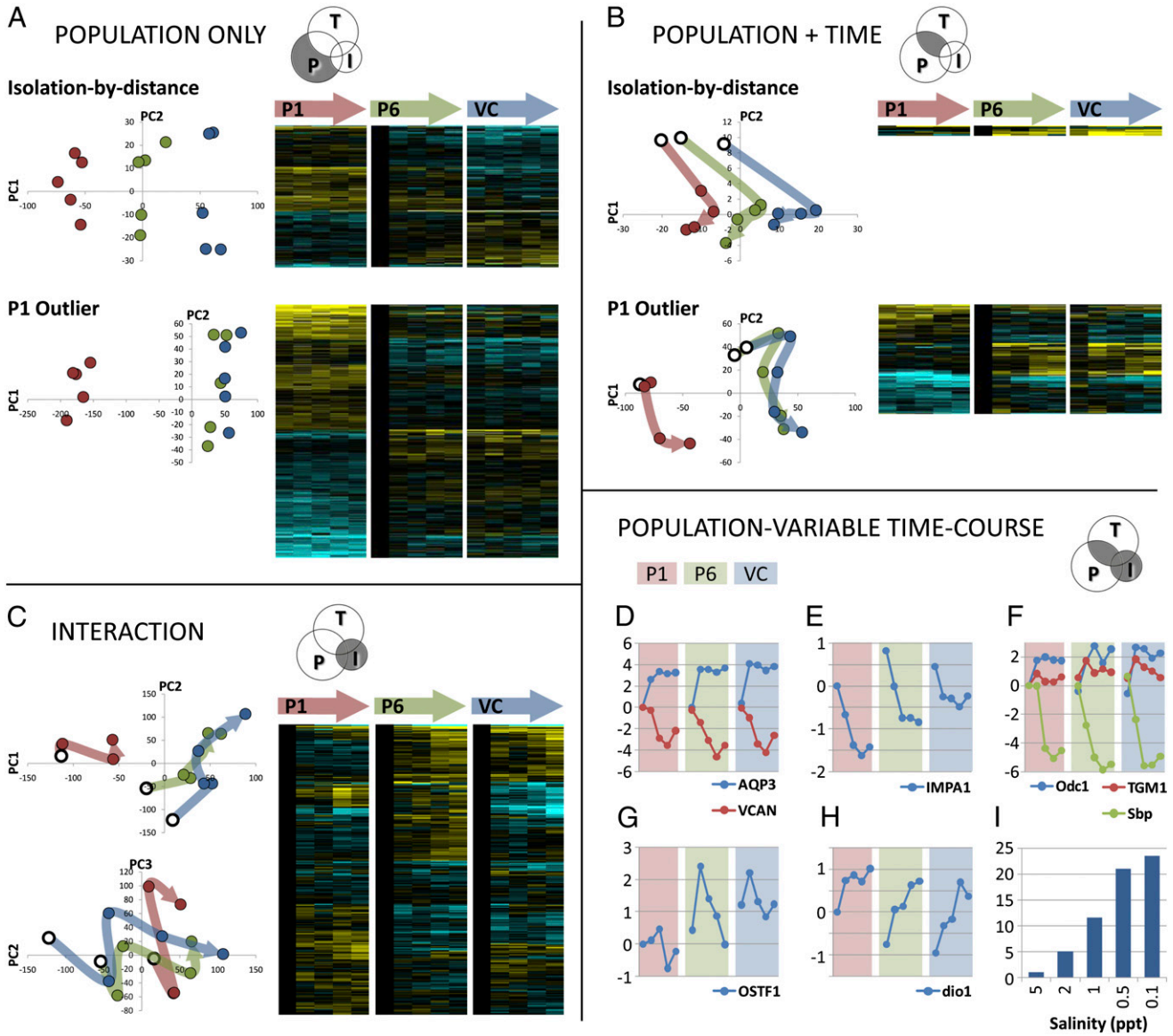


**Fig. 4.** Genes with population-variable expression. (*A*) Genes variable among populations only (no time effect). Top PC plot includes genes with population variation fitting the isolation-by-distance model where red, green, and blue circles represent sample time averages for populations P1, P6, and VC, respectively. Genes included are illustrated in the heatmap to the left of the PC plot, where rows are individual genes and columns are treatments, and the three blocks of columns represent the time-course expression level for populations P1, P6, and VC from left to right. The bottom PC plot and heatmap include genes with population variation fitting the P1-outlier model of population divergence. (*B*) Genes variable among populations and that change during acclimation. Those genes with patterns of population divergence that fit the isolation-by-distance model are represented by the top PC plot and heatmap, and those genes with divergence fitting the P1-outlier model represented by the bottom PC plot and heatmap pair. (*C*) PC plots (upper plot includes PC1 and PC2, lower plot includes PC2 and PC3) and heatmap for genes with expression patterns showing interaction between population and time. (*D*–H) Line graphs of average expression for individual genes (highlighted in the text) for each population (P1, P6, and VC represented by red, green, and blue, respectively) through consecutive time-points (starting at 0 h on the left, finishing at 168 h on the right, for each line), where *y* axis units represent $\log_2$-fold change in expression (each 1 unit = twofold expression change). (*I*) Bar graph show increasing expression of gene ODC1 at 6 h after transfer from 5 ppt (acclimation salinity) to successively lower salinities measured by qPCR.

**Population-Variable Genes.** Among the genes that are variable by population but not by time, 154 exhibit a pattern of population divergence consistent with the isolation-by-distance (neutral divergence) model, and 276 have a pattern of divergence supporting divergence only in our FW population (P1-outlier model) (Fig. 4*A*). In contrast, among the genes that are variable by both population and time, only 11 fit the neutral model, whereas 119 fit the model of biased FW population divergence (Fig. 4*B*). These data indicate that acclimation-enabling genes (insofar as genes that change in expression throughout the time-course are more likely to contribute to enabling physiological acclimation than those that do not change through the time-course) are more likely to exhibit nonneutral (putatively adaptive) patterns of population divergence than genes that are less likely to contribute to acclimation. That is, population-variable genes that change in expression during acclimation disproportionately fit the nonneutral FW population outlier model of divergence compared with population-variable genes that do not change in expression during acclimation (Fisher's exact test; $P < 0.001$). Indeed, genes showing footprints of directional selection between FW and marine sticklebacks are enriched for those known to be functionally involved in osmoregulation (26). Given

the ecological context of these populations (native habitats that are FW or salty) and the ecologically relevant physiological challenge (hypoosmotic challenge), this asymmetric divergence of hypoosmotic-induced gene expression in our FW population is consistent with asymmetric physiological divergence observed (Fig. 2).

The greatest population divergence in the trajectories of transcriptome change appears early in the acclimation response (Fig. 4 *B* and *C*). In our dataset, the genes that best represent such population divergence are those involved in cell-volume regulation, cell stabilization, and immediate early signal transduction (Fig. 4 *D–H*).

The immediate crisis encountered upon hypoosmotic challenge is swelling of gill cells and dilution of plasma osmolytes. Fish regulate cell volume by activating channel- and cotransporter-mediated efflux of osmolytes such as $Cl^-$ or $K^+$, allowing water to passively follow (27–29). Aquaporins are a family of proteins that facilitate passage of water molecules across biological membranes. Aquaporin 3 (AQP3) is one of the most dramatically up-regulated genes in our dataset (Fig. 4*D*), with expression quickly increasing up to 13-fold. In the P6 and VC populations, AQP3 expression peaks early at 6 h, whereas in the P1 population, the gene is less dramatically up-regulated and peaks later at 24 h. Concurrent with AQP3 increase is a decrease in expression of versican (VCAN) (Fig. 4*D*), a protein that contributes to cellular water retention by attracting cations (30), which again changed more quickly and dramatically in the P6 and VC populations. Inositol monophosphatase (IMPA1), which regulates the synthesis of the major osmolyte myo-inositol (31), also decreases in expression (Fig. 4*E*). IMPA1 is initially expressed at lower levels in the P1 population, so decreased expression is achieved more quickly in that population compared with P6 and VC. These data are consistent with substantially reduced cell volume disturbance in the P1 population relative to P6 and VC.

Several genes support the unique role of polyamine synthesis as an important early component of the compensatory response, and patterns of population variation in expression supports the P1-outlier model. Ornithine decarboxylase 1 (ODC1) is up-regulated upon hypoosmotic challenge (Fig. 4*F*), peaking quickly and more dramatically in the P6 and VC populations than in the P1 population. ODC1 catalyzes the first step in the synthesis of polyamines. Although polyamines are known to play a critical role in maintaining cell viability and growth under hypoosmotic conditions, for example in mammalian cells (32, 33), an apparent role of these molecules in the fish osmo-compensatory response is novel. Maintenance of protein conformation, protein–nucleic acid interactions, and protein synthesis depend critically on intracellular salt concentrations (particularly $Na^+/K^+$) (34–36), and polyamines help cells buffer these processes against changes in intracellular osmolytes (34). Given the rapid depletion of intracellular osmolytes during cell volume regulation (29, 37), up-regulation of polyamines is consistent with this protective function. Indeed, up-regulation of ODC1 is dose-responsive, where increasing severity of hypoosmotic challenge is associated with increased expression of ODC1 (Fig. 4*I*). Concurrent with ODC1 increase, spermine-binding protein (SBP) mRNA rapidly drops to nearly nondetectable levels within 24 h (Fig. 4*F*); this drop happens more rapidly and dramatically in P6 and VC populations. Presumably, increase in polyamine synthesis concurrent with decrease in polyamine binding would effectively increase free polyamines in the cell. Consistent with regulation of polyamines, we also observe increase in expression of transglutaminase-1 (TGM1) (Fig. 4*F*), which catalyzes the conjugation of polyamines to proteins (38).

Two genes that are likely components of the immediate-early response to osmotic challenge also exhibit population divergence that fits the P1-outlier model. Osmotic stress transcription factor 1 (OSTF1) is up-regulated quickly (Fig. 4*G*), peaking at 6 h in the two SW-derived populations P6 and VC but not up-regulated in the FW-tolerant P1 population. OSTF1 is an important component of the hyperosmotic response in fish gills (39), so the response to hypoosmotic shock that we demonstrate implies some function in initiating genomic response to osmotic shock in general. The lack of induction in the P1 population mirrors the absence of homeostatic imbalance after hypoosmotic challenge in this population, indicating that loss of osmotic balance is required to trigger OSTF1 induction. Deiodinase 1 (DIO1), which catalyzes the first step in thyroid hormone action, is also differentially up-regulated in our populations (Fig. 4*H*), where expression is initially much higher in the P1 population such that P3 and VC populations require 3 d to achieve transcript levels comparable with those reached by 6 h in P1. Although the role of thyroid hormone in osmoregulatory processes is controversial (40), DIO2 has been shown to harbor osmotic response elements in its promoter region in *F. heteroclitus* (41) and is up-regulated by hypoosmotic stress, and the thyroid signaling pathway is a target of adaptive divergence in FW populations of threespine sticklebacks (42).

Comparatively little is known about the mechanisms comprising the immediate-early responses of cells to osmotic stress relative to the mechanisms of downstream effectors of osmotic acclimation (43, 44). However, immediate-early transcriptional responses are highly correlated with the pattern of population variation in transcriptional trajectories during acclimation (Fig. 4) and better match the pattern of physiological divergence (Fig. 2) than the pattern of neutral genetic divergence (Fig. 1) observed between experimental populations.

## Conclusions

Evolutionary contrasts of transcriptome variation have been used to reveal the relative contributions of neutral and adaptive processes driving functional genome divergence in diverse taxa (reviewed in ref. 45) including killifish (46–48). However, these studies have tended to compare gene expression across taxa in static common-garden environments. In contrast, much functionally relevant variation is likely to be revealed within experimental designs that manipulate environmental conditions such that transcriptomewide norms of reaction can be compared across taxa (49–51). These designs, including the experiments presented here, promise to offer more nuanced insight into the functional relevance of genes with expression patterns that vary in response to the environment and vary across taxa from different native environments.

We find abrupt population genetic clines that bound a physiologically stressful salinity along parallel salinity gradients in killifish. These data are suggestive of adaptive divergence, and populations native to habitats on either side of this critical salinity exhibit diverged tolerance to osmotic challenge. We exploited this system to identify biochemical and physiological mechanisms that enable extreme physiological plasticity and to test how neutral and nonneutral evolutionary processes contribute to the divergence of acclimation-enabling gene expression. We find that population divergence in expression of acclimation-enabling genes is more likely to fit a nonneutral model of population divergence than for genes not involved in acclimation. These data indicate that natural selection is more likely to act on genes that are dynamically expressed in response to changing environments than on those that are not. Regulation of intracellular calcium, tight-junction proteins, nucleosome proteins, and energy metabolism represent core components of the hypoosmotic compensatory response. Importantly, the expression patterns of genes involved in polyamine regulation, cell volume regulation, and immediate early signaling highlight the critical importance of these pathways, because the degree of transcriptional response depends on the severity of osmotic stress, which differs across our experimental populations.

## Materials and Methods

**Population Genetics.** Capture locations for all fish are included in Table S1 ($n$ = 27–62 fish per site). Mitochondrial haplotype was determined by restriction digest of two PCR products within genes COII and ND5. Each fish was genotyped for each of eight microsatellite loci. For fixed sampling stations along

each river, we calculated the 20-y (1986–2005) average salinity and range. For experimental populations (P1, P6, and VC) we estimated pairwise genetic distance by using Cavalli-Sforza and Edwards' chord distance and calculated statistical significance by using a permutation procedure (1,000 X).

**Osmotic Challenge Experiments.** Fish were collected from sites P1, P6, and VC in June 2008 and maintained in recirculating aquarium systems at 32 ppt for at least 6 mo before exposures. Fish ($n = 6$) were sampled pretransfer, then transferred to experimental salinities (5.0, 0.4, and 0.1 ppt), including a 32 ppt control, and sampled at 6 h, 24 h, 72 h (3 d), 168 h (7 d), and 336 h (14 d) after transfer. Plasma osmolality was measured by freeze-point depression, plasma sodium by flame atomic absorption spectroscopy, and plasma chloride by using a modification of the mercuric thiocyanate method.

RNA isolation, microarray hybridizations, and data normalization are described in detail in *SI Materials and Methods*. A mixed model specifying "dye" as a fixed effect, "array" as a random effect, and time and population as main effects including an interaction term were used to identify genes differentially expressed ($P < 0.01$). Five individual fish (biological replicates) were included per treatment; when testing for significant treatment effects, the within-treatment variance is an estimate of interindividual variation. Genes with population-variable expression were assigned to a putatively neutral isolation-by-distance model if expression was significantly different between populations ($P < 0.01$) and most divergent between populations P1 and VC but of intermediate divergence between neighboring populations. Population-variable genes were assigned to the putatively adaptive "P1-outlier" model if expression was divergent between P1 and the other two populations ($P < 0.01$), but not different between P6 and VC ($P > 0.01$). Additional methods details can be found in *SI Materials and Methods*.

**ACKNOWLEDGMENTS.** We thank Jesse Hobson and John Waldron for assistance with field collections and laboratory exposures and Douglas Crawford and Marjorie Oleksiak for EST library construction and sequencing. Funding was from the National Science Foundation Grants EF-0723771 (to A.W. and F.G.) and BES-0652006 (to A.W.).

1. Whitehead A (2010) The evolutionary radiation of diverse osmotolerant physiologies in killifish (Fundulus sp.). *Evolution* 64:2070–2085.
2. Kaneko T, Katoh F (2004) Functional morphology of chloride cells in killifish Fundulus heteroclitus, a euryhaline teleost with seawater preference. *Fish Sci* 70:723–733.
3. Wood CM, Grosell M (2009) TEP on the tide in killifish (Fundulus heteroclitus): Effects of progressively changing salinity and prior acclimation to intermediate or cycling salinity. *J Comp Physiol B* 179:459–467.
4. Wood CM, Grosell M (2008) A critical analysis of transepithelial potential in intact killifish (Fundulus heteroclitus) subjected to acute and chronic changes in salinity. *J Comp Physiol B* 178:713–727.
5. Copeland DE (1950) Adaptive behavior of the chloride cell in the gill of Fundulus heteroclitus. *J Morphol* 87:369–379.
6. Philpott CW, Copeland DE (1963) Fine structure of chloride cells from three species of Fundulus. *J Cell Biol* 18:389–404.
7. Choe KP, et al. (2005) NHE3 in an ancestral vertebrate: Primary sequence, distribution, localization, and function in gills. *Am J Physiol Regul Integr Comp Physiol* 289: R1520–R1534.
8. Wilson JM, Laurent P (2002) Fish gill morphology: Inside out. *J Exp Zool* 293:192–213.
9. Kidder GW, 3rd, Petersen CW, Preston RL (2006) Energetics of osmoregulation: I. Oxygen consumption by Fundulus heteroclitus. *J Exp Zoolog A Comp Exp Biol* 305:309–317.
10. Kidder GW, 3rd, Petersen CW, Preston RL (2006) Energetics of osmoregulation: II. Water flux and osmoregulatory work in the euryhaline fish, Fundulus heteroclitus. *J Exp Zoolog A Comp Exp Biol* 305:318–327.
11. Bekkevold D, et al. (2005) Environmental correlates of population differentiation in Atlantic herring. *Evolution* 59:2656–2668.
12. McCairns RJS, Bernatchez L (2008) Landscape genetic analyses reveal cryptic population structure and putative selection gradients in a large-scale estuarine environment. *Mol Ecol* 17:3901–3916.
13. Evans DH, Piermarini PM, Choe KP (2005) The multifunctional fish gill: Dominant site of gas exchange, osmoregulation, acid-base regulation, and excretion of nitrogenous waste. *Physiol Rev* 85:97–177.
14. Whitehead A, Galvez F, Zhang S, Williams LM, Oleksiak MF (2010) Functional genomics of physiological plasticity and local adaptation in killifish. *J Hered* 10.1093/jhered/esq077.
15. Hughes I, et al. (2004) Otopetrin 1 is required for otolith formation in the zebrafish Danio rerio. *Dev Biol* 276:391–402.
16. Hughes I, Saito M, Schlesinger PH, Ornitz DM (2007) Otopetrin 1 activation by purinergic nucleotides regulates intracellular calcium. *Proc Natl Acad Sci USA* 104: 12023–12028.
17. Marshall WS, Grosell M (2005) Ion transport, osmoregulation, and acid-base balance. *Physiology of Fishes*, eds Evans DH, Claiborne JB (CRC, Boca Raton, FL), pp 177–230.
18. Matter K, Balda MS (2003) Functional analysis of tight junctions. *Methods* 30:228–234.
19. Van Itallie CM, Anderson JM (2004) The molecular physiology of tight junction pores. *Physiology (Bethesda)* 19:331–338.
20. Patrick ML, Part P, Marshall WS, Wood CM (1997) Characterization of ion and acid-base transport in the fresh water adapted mummichog (Fundulus heteroclitus). *J Exp Zool* 279:208–219.
21. Scott GR, Rogers JT, Richards JG, Wood CM, Schulte PM (2004) Intraspecific divergence of ionoregulatory physiology in the euryhaline teleost Fundulus heteroclitus: possible mechanisms of freshwater adaptation. *J Exp Biol* 207:3399–3410.
22. Bagherie-Lachidan M, Wright SI, Kelly SP (2008) Claudin-3 tight junction proteins in Tetraodon nigroviridis: cloning, tissue-specific expression, and a role in hydromineral balance. *Am J Physiol Regul Integr Comp Physiol* 294:R1638–R1647.
23. Evans DH, Piermarini PM, Potts WTW (1999) Ionic transport in the fish gill epithelium. *J Exp Zool* 283:641–652.
24. Laurent P, Chevalier C, Wood CM (2006) Appearance of cuboidal cells in relation to salinity in gills of Fundulus heteroclitus, a species exhibiting branchial Na+ but not Cl- uptake in freshwater. *Cell Tissue Res* 325:481–492.
25. Ahmed S, Brickner JH (2007) Regulation and epigenetic control of transcription at the nuclear periphery. *Trends Genet* 23:396–402.
26. Shimada Y, Shikano T, Merila J (2011) A high incidence of selection on physiologically important genes in the three-spined stickleback, Gasterosteus aculeatus. *Mol Biol Evol* 28:181–193.
27. Hoffmann EK, Schettino T, Marshall WS (2007) The role of volume-sensitive ion transport systems in regulation of epithelial transport. *Comp Biochem Physiol A Mol Integr Physiol* 148:29–43.
28. Marshall WS, Ossum CG, Hoffmann EK (2005) Hypotonic shock mediation by p38 MAPK, JNK, PKC, FAK, OSR1 and SPAK in osmosensing chloride secreting cells of killifish opercular epithelium. *J Exp Biol* 208:1063–1077.
29. Avella M, Ducoudret O, Pisani DF, Poujeol P (2009) Swelling-activated transport of taurine in cultured gill cells of sea bass: Physiological adaptation and pavement cell plasticity. *Am J Physiol Regul Integr Comp Physiol* 296:R1149–R1160.
30. Faggian J, Fosang AJ, Zieba M, Wallace MJ, Hooper SB (2007) Changes in versican and chondroitin sulfate proteoglycans during structural development of the lung. *Am J Physiol Regul Integr Comp Physiol* 293:R784–R792.
31. Michell RH (2008) Inositol derivatives: Evolution and functions. *Nat Rev Mol Cell Biol* 9:151–161.
32. Poulin R, Wechter RS, Pegg AE (1991) An early enlargement of the putrescine pool is required for growth in L1210 mouse leukemia cells under hypoosmotic stress. *J Biol Chem* 266:6142–6151.
33. Rhee HJ, Kim EJ, Lee JK (2007) Physiological polyamines: Simple primordial stress molecules. *J Cell Mol Med* 11:685–703.
34. Capp MW, et al. (1996) Compensating effects of opposing changes in putrescine (2+) and K+ concentrations on lac repressor-lac operator binding: in Vitro thermodynamic analysis and in vivo relevance. *J Mol Biol* 258:25–36.
35. Prabhu N, Sharp K (2006) Protein-solvent interactions. *Chem Rev* 106:1616–1623.
36. Shinohara T, Piatigorsky J (1977) Regulation of protein synthesis, intracellular electrolytes and cataract formation in vitro. *Nature* 270:406–411.
37. Hoffmann EK (1992) Cell swelling and volume regulation. *Can J Physiol Pharmacol* 70 (Suppl):S310–S313.
38. Greenberg CS, Birckbichler PJ, Rice RH (1991) Transglutaminases: Multifunctional cross-linking enzymes that stabilize tissues. *FASEB J* 5:3071–3077.
39. Fiol DF, Kültz D (2005) Rapid hyperosmotic coinduction of two tilapia (Oreochromis mossambicus) transcription factors in gill cells. *Proc Natl Acad Sci USA* 102:927–932.
40. McCormick SD (2001) Endocrine control of osmoregulation in teleost fish. *Am Zool* 41: 781–794.
41. López-Bojórquez L, Villalobos P, García-G C, Orozco A, Valverde-R C (2007) Functional identification of an osmotic response element (ORE) in the promoter region of the killifish deiodinase 2 gene (FhDio2). *J Exp Biol* 210:3126–3132.
42. Kitano J, et al. (2010) Adaptive divergence in the thyroid hormone signaling pathway in the stickleback radiation. *Curr Biol* 20:2124–2130.
43. Evans TG, Somero GN (2008) A microarray-based transcriptomic time-course of hyper- and hypoosmotic stress signaling events in the euryhaline fish Gillichthys mirabilis: Osmosensors to effectors. *J Exp Biol* 211:3636–3649.
44. Fiol DF, Chan SY, Kültz D (2006) Identification and pathway analysis of immediate hyperosmotic stress responsive molecular mechanisms in tilapia (Oreochromis mossambicus) gill. *Comp Biochem Physiol Part D Genomics Proteomics* 1:344–356.
45. Whitehead A, Crawford DL (2006) Variation within and among species in gene expression: Raw material for evolution. *Mol Ecol* 15:1197–1211.
46. Fisher MA, Oleksiak MF (2007) Convergence and divergence in gene expression among natural populations exposed to pollution. *BMC Genomics* 8:108.
47. Oleksiak MF, Churchill GA, Crawford DL (2002) Variation in gene expression within and among natural populations. *Nat Genet* 32:261–266.
48. Whitehead A, Crawford DL (2006) Neutral and adaptive variation in gene expression. *Proc Natl Acad Sci USA* 103:5425–5430.
49. Aubin-Horth N, Renn SCP (2009) Genomic reaction norms: Using integrative biology to understand molecular mechanisms of phenotypic plasticity. *Mol Ecol* 18:3763–3780.
50. Lockwood BL, Sanders JG, Somero GN (2010) Transcriptomic responses to heat stress in invasive and native blue mussels (genus Mytilus): Molecular correlates of invasive success. *J Exp Biol* 213:3548–3558.
51. Whitehead A, Triant DA, Champlin D, Nacci D (2010) Comparative transcriptomics implicates mechanisms of evolved pollution tolerance in a killifish population. *Mol Ecol* 19:5186–5203.